

# Charge mobility determination by current extraction under linear increasing voltages: the case of non-equilibrium charges and field-dependent mobilities

Sebastian Bange,<sup>1,\*</sup> Marcel Schubert,<sup>1</sup> and Dieter Neher<sup>1</sup>

<sup>1</sup>*Universität Potsdam, Institut für Physik und Astronomie,  
Karl-Liebknecht-Str. 24-25, 14476 Potsdam-Golm, Germany*

(Dated: February 3, 2022)

## Abstract

The method of current extraction under linear increasing voltages (CELIV) allows for the simultaneous determination of charge mobilities and charge densities directly in thin films as used in organic photovoltaic cells (OPV). In the past, it has been specifically applied to investigate the interrelation of microstructure and charge transport properties in such systems. Numerical and analytical calculations presented in this work show that the evaluation of CELIV transients with the commonly used analysis scheme is error prone once charge recombination and, possibly, field dependent charge mobilities are taken into account. The most important effects are an apparent time-dependence of charge mobilities and errors in the determined field dependencies. Our results implicate that reports on time-dependent mobility relaxation in OPV materials obtained by the CELIV technique should be carefully revisited and confirmed by other measurement methods.

## I. INTRODUCTION

The understanding of charge transport properties of organic semiconducting materials is one of the keys for further improvement of devices such as organic light-emitting diodes and organic photovoltaic cells. Owing to its simplicity, straightforward data analysis and applicability to measurements on films of well below 100 nm thickness, the technique of current extraction by linear increasing voltages (CELIV, see Ref. 1) has attracted considerable interest over the past few years. Its unique attractiveness stems from the opportunity to study charge transport directly in thin film systems as used in the actual devices. As such, it is the ideal technique to investigate structure-property relationships of charge transport and recombination e.g. in state-of-the-art donor/acceptor photovoltaic systems such as polymer/polymer and polymer/small molecule material blends, the morphology of which cannot be well reproduced in modified sample geometries. CELIV has been originally introduced to determine charge mobility and concentration in microcrystalline Si:H semiconductors and doped conjugated polymers under thermal equilibrium conditions,<sup>1,2</sup> but was later applied to study the field-dependent mobility of non-equilibrium charge carriers created by the absorption of a light pulse.<sup>3,4,5</sup> Hereby photo-CELIV experiments have been used to quantify the decay of carrier density with time and to measure the time dependence of mobility. Time-dependent relaxation of charge mobilities as determined by the photo-CELIV technique has been reported for various state-of-the-art photovoltaic bulk heterojunction blends.<sup>6,7,8,9,10</sup> It has usually been attributed to the relaxation of carrier energies in an extended density of transport states present in these disordered solids.

This paper treats the analytic and numerical analysis of CELIV experiments under conditions diverging from the equilibrium assumptions of its original derivation. We first review the basic theory of equilibrium CELIV experiments and point out inaccuracies in the original derivations. Based on this, we treat the case of non-equilibrium photogenerated charge carriers with constant mobility by both numerical as well as analytical methods. We show that with the standard evaluation scheme applied under this condition, an apparently time-dependent charge mobility is deduced that is solely the effect of the used analysis. We provide an analytic analysis method to determine charge mobilities in a reliable way even under conditions of non-equilibrium charge carrier recombination. Finally, we treat the application of CELIV measurements to the situation of field-dependent carrier mobilities. A

modified analysis method is introduced and shown to result in significantly reduced errors for the derived field dependence.

## II. CHARGE MOBILITY DETERMINATION BY THE CELIV TECHNIQUE

The experimental procedure and analytic evaluation for CELIV experiments has been introduced by Juska et al. in Ref. 1, to which the reader is referred for further details. Consider the extraction of equilibrium charge carriers of density  $n$  and mobility  $\mu$  in the electric field  $U/d$ , where  $d$  is the layer thickness and  $U(t) = U't$  is the applied voltage that rises linearly in time. Without restriction of the generality of our analysis, we assume that the internal electric field is zero at  $U = 0$ . This differs from the more general situation where electrodes of different work functions are used. Note that experimentally one should account for the built-in potential due to differences in the electrode work functions to ensure that the electric field within the organic layer is zero at  $U = 0$ . Assuming that the electrode area  $A$  is much larger than  $d$ , that one carrier type is much more mobile than the other (here: holes) and that the electrodes are non-injecting, the time dependent charge density is  $\rho(z, t) = -en$  for  $0 \leq z \leq l(t)$  and  $\rho(z, t) = 0$  for  $l(t) < z < d$ . Hereby, all holes have been depleted from the layer up to the time-dependent extraction depth  $l(t)$ . The current density measured in the external circuit due to the extraction of charges at  $z = d$  is

$$j = \frac{\epsilon}{d}U' + \begin{cases} \frac{en}{d} \left(1 - \frac{l}{d}\right) \left(\mu U't - \frac{en\mu l^2}{2\epsilon}\right) & (l(t) \leq d) \\ 0 & \text{else,} \end{cases} \quad (1)$$

assuming  $t \gg RC$  where  $R$  is the external circuit resistance and  $C = \epsilon A/d$  is the geometrical sample capacitance assuming a permittivity of  $\epsilon = \epsilon_r \epsilon_0$ . The extraction depth is the solution of

$$\frac{dl(t)}{dt} + \frac{en\mu l^2(t)}{2d\epsilon} = \frac{\mu U't}{d} \quad (2)$$

under the initial conditions  $l(0) = 0$  and  $dl(0)/dt = 0$ . This is a first order nonlinear differential equation of Ricatti type that can be solved numerically parametric in the dimensionless voltage slope  $\epsilon^2 U'/2e^2 n^2 \mu d^2$ . At some time  $t_{\max}$ , the current density (1) will peak at  $j(t_{\max})$ , where the relative height  $\Delta j/j = (j(t_{\max}) - j(0))/j(0)$  can be expressed as a bijective function of the dimensionless parameter  $\chi = \mu U't_{\max}^2/2d^2$ . Figure 1 shows the result of our numerical calculation of  $\chi$  as a function of  $\Delta j/j(0)$ .  $\chi$  is equal to 1/3 at

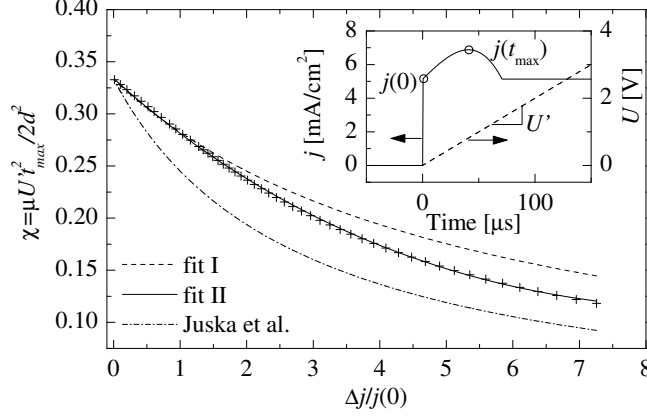


FIG. 1: Results of the calculation of  $\chi$  as function of  $\Delta j/j(0)$  from the numerical solution of equations (1) and (2) (symbols), compared to fit I and II as discussed in the text as well as the parametrisation used by Juska et al. in Ref. 2. The inset shows a typical CELIV current calculated for  $d = 100$  nm,  $U' = 2 \times 10^4$  V/s,  $\mu = 2 \times 10^6$  cm<sup>2</sup>/Vs,  $n = 10^{22}$  m<sup>-3</sup>,  $A = 1$  mm<sup>2</sup> and  $\epsilon_r = 2.9$ , indicating the capacitive charging current  $j(0)$  and the maximum current  $j(t_{\max})$ .

$\Delta j/j(0) = 0$  and decreases in a nonlinear fashion for  $\Delta j/j(0) > 0$ . Also shown in figure 1 are two different parametrizations of this curve in terms of  $\chi = [3(1 + 0.18\Delta j/j(0))]^{-1}$  (fit I) and  $\chi = 0.329 \exp[-0.180\Delta j/j(0)] + 0.005 \exp[0.253\Delta j/j(0)]$  (fit II) which are good approximations for  $\Delta j/j(0) \leq 1$  or  $\Delta j/j(0) \leq 7$  for fit I and fit II, respectively. Using these, the charge mobility can be calculated as  $\mu = 2d^2\chi/U't_{\max}^2$ , resulting in

$$\mu = \frac{2d^2}{3U't_{\max}^2(1 + 0.18\frac{\Delta j}{j(0)})} \quad (3)$$

when using fit I valid for  $\Delta j/j(0) \leq 1$  or

$$\mu = \frac{2d^2}{U't_{\max}^2} \left( 0.329e^{-0.180\frac{\Delta j}{j(0)}} + 0.005e^{0.253\frac{\Delta j}{j(0)}} \right) \quad (4)$$

when using fit II valid for  $\Delta j/j(0) \leq 7$ . This is in variance with the result published by Juska et al.<sup>2,11</sup> and used in several articles,<sup>6,12,13</sup> which corresponds to choosing  $\chi = [3(1 + 0.36\Delta j/j(0))]^{-1}$ . In order to provide an independent test for the consistency of our analysis, we simulated the CELIV experiment with a numerical drift-diffusion solver program. Figure 2 shows the resulting current transients assuming a charge mobility of  $\mu = 2 \times 10^{-6}$  cm<sup>2</sup>/Vs, a layer thickness of  $d = 65$  nm with  $\epsilon_r = 3$ , a voltage slope of  $U' = 2 \times 10^4$  V/s and an initial charge carrier density of  $n = 4 \times 10^{22}$  m<sup>-3</sup>. As expected, the numerically evaluated solution to equations (1) and (2) closely follows the simulation results

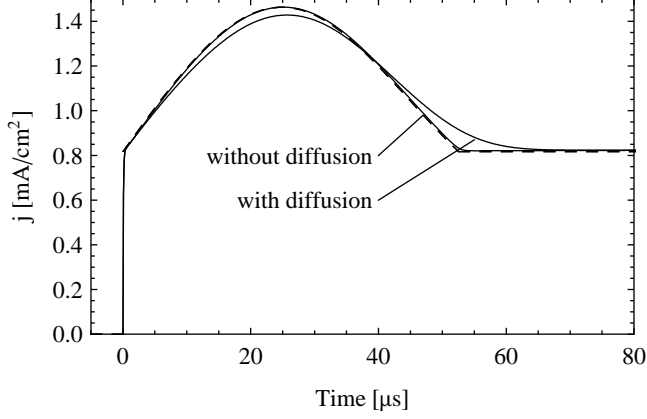


FIG. 2: Numerically simulated CELIV transients (solid lines), for simulation parameters see text. The results are shown both with and without charge diffusion according to the Einstein relation. The dashed line corresponds to the numerical solution of equations (1) and (2) and closely follows the simulation results excluding charge diffusion.

when charge diffusion is suppressed. We determined  $\Delta j/j(0) = 0.781$  and  $t_{\max} = 25.125 \mu\text{s}$  from the simulation data, from which the apparent mobilities  $\mu = 1.96 \times 10^6 \text{ cm}^2/\text{Vs}$  and  $\mu = 1.95 \times 10^6 \text{ cm}^2/\text{Vs}$  are calculated using equation (3) or equation (4), respectively. Using the Juska et al. result, we instead obtain  $\mu = 1.74 \times 10^6 \text{ cm}^2/\text{Vs}$ , which proves that this approximation underestimates the mobility. We therefore suggest to calculate the mobility using equation (3) or (4), depending on the magnitude of  $\Delta j/j(0)$ .

### III. THE ROLE OF BIMOLECULAR CHARGE RECOMBINATION

The gaussian disorder model of charge transport in organic semiconductors predicts that after photoexcitation, charge carriers will relax energetically towards their equilibrium energy, with a concomitant mobility decrease. The understanding of this process is of considerable importance for organic photovoltaic devices in order to further improve their efficiency. Recently, the CELIV method has been applied to the study of non-equilibrium charge carriers photogenerated by the absorption of short laser pulses.<sup>3,4</sup> Various publications used this photo-CELIV technique to study both mobility and density relaxation of photogenerated carriers.<sup>5,6,7,12,13</sup> We feel that it is important to point out that the analytic equations used to evaluate CELIV experiments have been derived by assuming the presence of *equilibrium* carriers. Thus, bimolecular charge recombination has not been taken into account

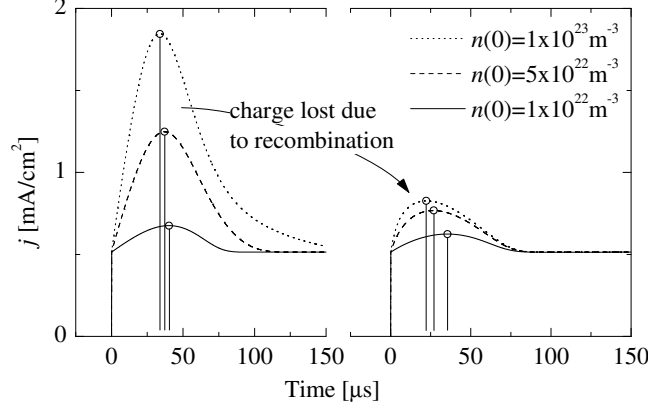


FIG. 3: Comparison of numerically simulated CELIV current transients without (left) and with (right) bimolecular charge recombination according to the Langevin mechanism, for simulation parameters see text. The results are shown parametric in the initial charge density, the position of  $j(t_{\max})$  is marked by a circle and vertical line.

for the calculation of the time-dependent charge density  $\rho(z, t)$ . However, assuming charge recombination according to the Langevin mechanism<sup>14</sup>, the charge density at  $z > l(t)$  decays as  $n(t) = n(0)(1 + t/\tau_\sigma)^{-1}$ , where  $\tau_\sigma = \epsilon/en(0)\mu$  is the dielectric relaxation time. This renders the evaluation of CELIV experiments in terms of equation (4) inaccurate and motivates to study the effects of charge recombination by numerical simulations. Figure 3 shows the results of numerically simulated current transients assuming  $\mu = 2 \times 10^6$  V/m,  $d = 100$  nm,  $\epsilon_r = 3$  and  $U' = 2 \times 10^4$  V/s while varying the initial charge density  $n(0)$  between  $10^{22}$  m<sup>-3</sup> and  $10^{23}$  m<sup>-3</sup>. When bimolecular charge recombination is taken into account in the simulations, a significantly reduced amount of charges is extracted, reducing  $\Delta j/j(0)$  and strongly shifting  $t_{\max}$  towards shorter times. Thus, the apparent mobilities calculated from transients affected by recombination using equation (4) are expected to be higher compared to those calculated from recombination-free transients. We analyzed this in more detail for polymer blends of poly[2,5-dimethoxy-1,4-phenylenevinylene-2-methoxy-5-(2-ethylhexyloxy)-1,4-phenylenevinylene] (M3EH-PPV) with poly[oxa-1,4-phenylene-1,2-(1-cyano)-ethylene-2,5-dioctyloxy-1,4-phenylene-1,2-(2-cyano)-ethylene-1,4-phenylene] (CN-ether-PPV), for details of these materials see Ref. 8. Samples were fabricated by spin-coating a 1:1 blend of these polymers from chlorobenzene solution onto precleaned and structured ITO substrates covered by a layer of PEDOT:PSS (Clevios AI4083 obtained

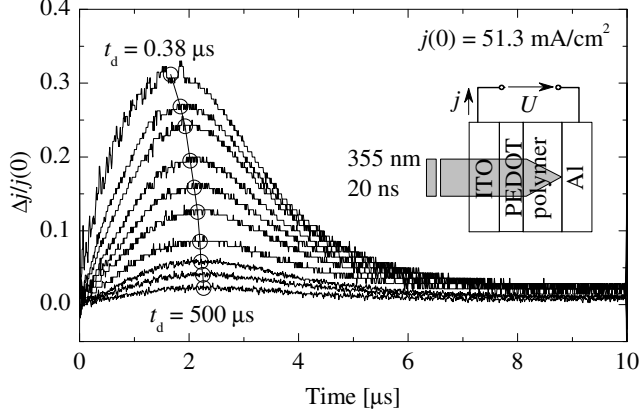


FIG. 4: CELIV current transients measured for a 55 nm thick M3EH-PPV:CN-ether-PPV blend layer at  $U' = 1.06 \text{ V}/\mu\text{s}$  for different delay times after photoexcitation ranging from near zero up to 500  $\mu\text{s}$ . Connected circles indicate the determined  $j(t_{\text{max}})$  points. The inset schematically shows the layer structure and illumination direction used for the experiment.

from H.C. Starck, Germany) and evaporating a 200 nm thick aluminum top electrode. Devices were fabricated under protective nitrogen atmosphere and encapsulated by a cover glass and two-component epoxy resin prior to measurements under ambient conditions. Figure 4 shows photo-CELIV current transients obtained for a device with a 55 nm thick polymer layer and an electrode area of  $A = 1 \text{ mm}^2$  at a voltage slope of  $U' = 1.06 \text{ V}/\mu\text{s}$  for various delay times  $t_d$  between photogeneration using a 20 ns long laser pulse of 355 nm wavelength and the beginning of charge extraction. As is obvious from the current transients, the time  $t_{\text{max}}$  of maximum extraction current strongly shifts to smaller values for short  $t_d$ . We modeled the impact of charge density on these measurement results by numerical simulation of the experiment using the model parameters  $d = 55 \text{ nm}$ ,  $U' = 1.06 \text{ V}/\mu\text{s}$ ,  $\epsilon = 3$  and assuming a field- and time-independent mobility  $\mu = 3.8 \times 10^{-6} \text{ cm}^2/\text{Vs}$ . The charge density  $n(0)$  at the beginning of charge extraction was varied between  $10^{21} \text{ m}^{-3}$  and  $10^{25} \text{ m}^{-3}$ . Figure 5 shows the  $\Delta j/j(0)$  and apparent mobilities calculated from the simulated CELIV transients using equation (4). The apparent mobility (solid symbols) rises with charge density for  $n(0) > 10^{23} \text{ m}^{-3}$ , corresponding to current maxima (open symbols) of  $\Delta j/j(0) > 0.1$ . It has been suggested<sup>15</sup> that CELIV transients are most convenient to determine experimentally when  $\Delta j/j(0) \approx 1$ . Our simulations strongly discourage this choice whenever nonequilibrium charge carriers are investigated, since charge recombination

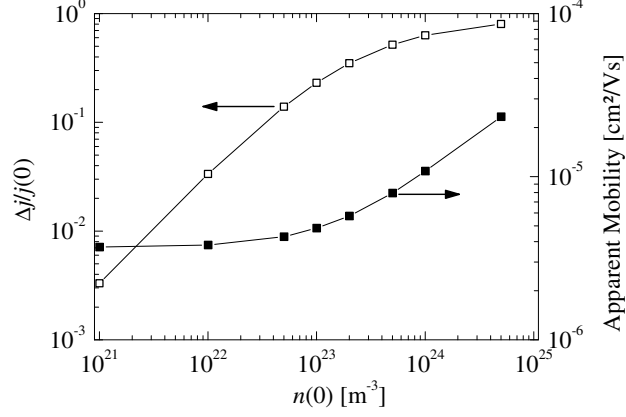


FIG. 5: Analysis of numerically simulated CELIV transients in terms of current maximum  $\Delta j/j(0)$  (open symbols) and apparent mobility (solid symbols) calculated from equation (4) for a range of charge densities  $n(0)$  present at the beginning of charge extraction ( $t_d = 0$ ). The simulation model parameters correspond to the experimental situation of figure 4.

strongly distorts the transients in this regime. The simulation data can also be calculated by varying the delay time  $t_d$  between photogeneration of charge carriers of density  $n_{\text{photo}}$  and charge extraction, whereby the charge density at the beginning of charge extraction is  $n(0) = n_{\text{photo}}/(1 + e\mu n_{\text{photo}}t/\epsilon)$ . Figure 6 compares the apparent mobilities calculated from simulation data using equation (4) with those obtained in the same way from figure 4. Under the assumption of  $n_{\text{photo}} = 4 \times 10^{23} \text{ m}^{-3}$ , simulated results closely follow those obtained from the measurement over the whole range of delay times. For the shortest delay time, we estimate from the experimental current transient that a total amount of charges corresponding to a charge density of only  $5 \times 10^{22} \text{ m}^{-3}$  could be extracted during the CELIV experiments. For the simulated transients at a comparable delay time of  $t_d = 0.38 \mu\text{s}$  we calculated a very similar value of  $6 \times 10^{22} \text{ m}^{-3}$ . Thus, more than 80% of the initially generated charge pairs are lost due to bimolecular recombination during the delay time and the initial part of the CELIV transient.

Since the effect of charge recombination during non-equilibrium CELIV experiments is of considerable experimental interest, we will elaborate further on an analytic treatment of this situation. In general, the charge density  $\rho$  will follow a complicated spatial and time dependence, since charge recombination will take place only in the region  $z > l(t)$ , where both charge types are present. To keep our analysis sufficiently general, we consider the case



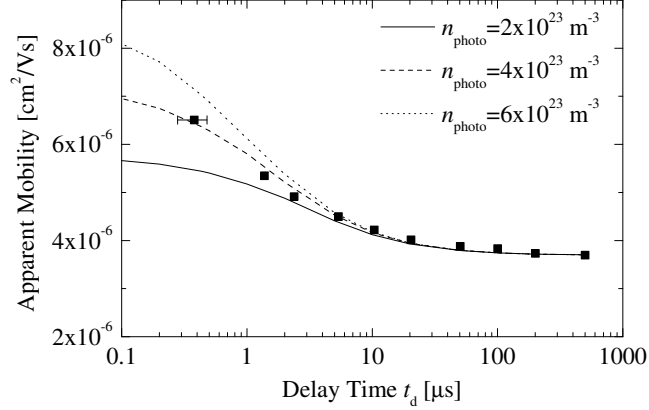


FIG. 6: Apparent mobility calculated from the experimental CELIV transients shown in figure 4 using equation (4) (symbols), compared with the results of numerical simulations assuming various photogenerated charge carrier densities  $n_{\text{photo}}$ , a time-independent charge mobility  $\mu = 3.8 \times 10^{-6} \text{ cm}^2/\text{Vs}$  and bimolecular recombination according to the Langevin mechanism. Data is shown as a function of the delay time  $t_d$  between photoexcitation and the beginning of the extraction voltage pulse, the approximate uncertainty of delay time for first data point is indicated by error bars.

of a dielectric relaxation time given by  $\tau_\sigma = \epsilon/en(0)\mu\beta$ , where  $\beta$  is a recombination prefactor ( $\beta = 1$  corresponds to Langevin recombination). Reduced bimolecular recombination with  $\beta \ll 1$  has been shown to prevail in some polymer/small molecule donor/acceptor blend solar cell materials.<sup>16</sup> The spatial charge distribution for  $z \leq l(t)$  then depends on  $l(t)$  as

$$\rho(z) = \frac{-en_0}{1 + \tau_\sigma^{-1}l^{(-1)}(z)}, \quad (5)$$

where  $l(l^{(-1)}(z)) = z$  defines the inverse function  $l^{(-1)}(z)$  of  $l(t)$ . Despite this implicit expression for the charge density, analysis shows that the current transient can be obtained by the surprisingly simple expression

$$j = \frac{\epsilon}{d}U' + en\frac{1 - l/d}{1 + t/\tau_\sigma} \frac{dl(t)}{dt}. \quad (6)$$

The time dependence of  $l(t)$  is calculated from

$$\frac{d^2l(t)}{dt^2} = \frac{\mu U'}{d} - \frac{1}{d\beta\tau_\sigma} \frac{l(t)}{1 + t/\tau_\sigma} \frac{dl(t)}{dt}, \quad (7)$$

the solution of which converges to that of equation (2) for  $\beta \rightarrow 0$ . We compared this solution to the results of numerical simulations and found good agreement when charge diffusion was

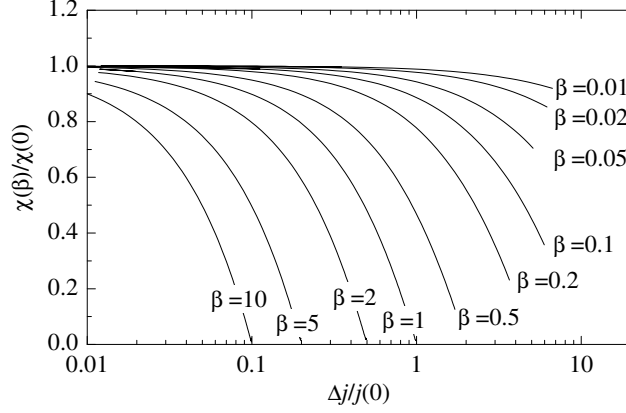


FIG. 7: Results of the calculation of  $\chi(\beta)/\chi(0)$  as function of  $\Delta j/j(0)$  from the numerical solution of equations (6) and (7), parametric in the bimolecular recombination prefactor  $\beta$ .

neglected in the simulations. Using the same techniques as for figure 1, we calculated  $\chi$  as a function of  $\Delta j/j(0)$  parametric in the prefactor  $\beta$ . Figure 7 plots the results relative to  $\chi$  as determined for  $\beta = 0$ . Given a specific recombination prefactor  $\beta$ , these curves can be used to directly extract the recombination-corrected charge mobility from the measurement or to estimate the impact of recombination on CELIV results obtained by the more simple estimates provided by equations (3) and (4). We additionally fitted  $\chi$  as a function of  $\Delta j/j(0)$  for the case  $\beta = 1$  by the double exponential expression used above. This directly results in the expression

$$\mu = \frac{2d^2}{U't_{\max}^2} \left( 0.860e^{-0.486\frac{\Delta j}{j(0)}} - 0.525e^{0.0077\frac{\Delta j}{j(0)}} \right) \quad (8)$$

which is valid at  $\Delta j/j(0) < 0.95$  with a relative error of less than 3.5% and can be used to determine true charge mobilities from CELIV transients even under conditions of high charge densities, assuming that Langevin recombination prevails.

#### IV. FIELD-DEPENDENT CHARGE MOBILITIES

The charge mobility in organic semiconductors is usually considered to be both a field and density dependent quantity, where the electric field dependence has been experimentally found to mostly follow a Poole-Frenkel type law  $\mu(E) = \mu_0 \exp(\kappa\sqrt{E})$ . The work of Bäessler et al. has shown that this can be understood in terms of transport sites having random energies according to a gaussian distribution, rendering  $\mu_0$  and  $\kappa$  temperature dependent.<sup>17</sup> CELIV

experiments provide a unique opportunity to determine charge mobilities in undoped organic semiconductor films of well below 100 nm thickness, but has the disadvantage of working under conditions of a non-constant electric field. Since the mobility is calculated from the maximum extraction current point, the determined values have usually been associated with the electric field  $E^* = U't_{\max}/d$  (*extraction field*) present at the time of maximum extraction current,<sup>5,7,18</sup> although the validity of this approach has never been tested rigorously. As we have shown above, mobilities determined for non-equilibrium charge carriers using photo-CELIV are more reliable when  $\Delta j/j(0) \ll 1$ , i.e. when  $\tau_\sigma \gg t_{\text{tr}}$  where  $t_{\text{tr}} = d\sqrt{2/\mu U'}$  is the charge transit time through the layer. Under this approximation, the current density (1) becomes

$$j = \frac{\epsilon}{d}U' + \frac{en}{d} \left(1 - \frac{l}{d}\right) U't\mu_0 e^{\kappa^*} \quad (9)$$

for  $l(t) \leq d$ , where

$$l(t) = \frac{2\mu_0}{U'\kappa^4} [6d + 6de^{\kappa^*}(\kappa^* - 1) + U't\kappa^2 e^{\kappa^*}(\kappa^* - 3)], \quad (10)$$

and  $\kappa^*(t) = \kappa\sqrt{U't/d}$ . Unfortunately, equation (9) does not provide any closed analytic expression for  $t_{\max}$  and  $\Delta j/j(0)$ , but can be evaluated numerically. Figure 8 compares the apparent charge mobility calculated from such data using equation (3) to the actual mobility at  $E = E^* = U't_{\max}/d$ . These results were calculated for  $\mu_0 = 10^{-6} \text{ cm}^2/\text{Vs}$ ,  $d = 100 \text{ nm}$  and  $\epsilon_r = 3$ , but are considered to be fairly general since they are independent of  $n$  at sufficiently low densities and invariant under the mutual transformation  $\mu_0 \rightarrow \alpha\mu_0$ ,  $U' \rightarrow \alpha U'$  for arbitrary  $\alpha$ . It is obvious that significant errors in the apparent mobility occur at large  $\kappa$  and large  $U'$ . We propose a simple improvement of the CELIV analysis by attributing the apparent mobility values to the extraction field redefined as  $E^* = 0.65 \cdot U't_{\max}/d$ . The corresponding relative error of the apparent mobility is also shown in figure 8 and stays within 20% in the relevant parameter regime. In order to test this approach, we numerically simulated CELIV transients in the  $\Delta j/j(0) \ll 1$  regime for various values of  $U'$ , assuming  $d = 100 \text{ nm}$ ,  $\epsilon_r = 3$ ,  $\mu_0 = 10^{-6} \text{ cm}^2/\text{Vs}$  and  $\kappa = 10^{-3} (\text{m/V})^{1/2}$ . Figure 9 compares the apparent mobility values determined according to equation (3) and associated with either choice of  $E^*$ . We found that using  $E^* = 0.65 \cdot U't_{\max}/d$  generally gives better results for this type of field dependence. The experimental error can be further minimized by using an iterative procedure if the field-dependence of the apparent mobility indeed follows the Poole-Frenkel behaviour: (1.) measure CELIV transients at different  $U'$  to obtain a range

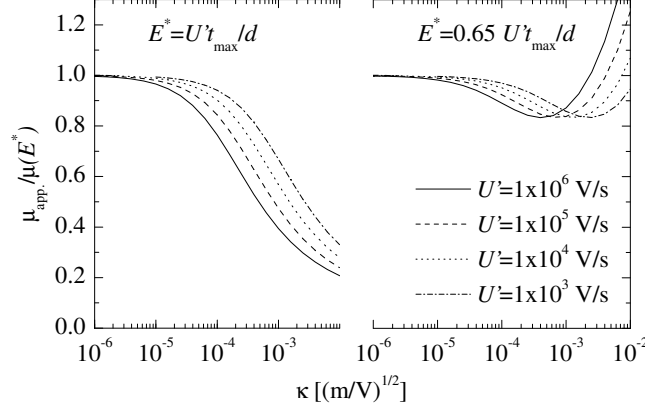


FIG. 8: Ratio of the apparent mobility  $\mu_{\text{app}}$  and the actual mobility at the electric field of  $E^* = U't_{\text{max}}/d$  (left) and  $E^* = 0.65 \cdot U't_{\text{max}}/d$  (right) as function of the Poole-Frenkel parameter  $\kappa$ . The apparent mobility was calculated from the current transients given by equation (9) using  $\mu_0 = 10^{-6} \text{ cm}^2/\text{Vs}$ ,  $d = 100 \text{ nm}$  and  $\epsilon_r = 3$  by applying equation (3) and is shown parametric in the voltage slope  $U'$ .

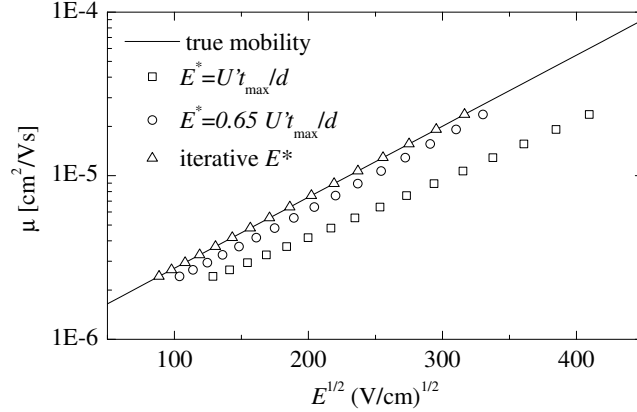


FIG. 9: Apparent charge mobilities calculated from simulated CELIV transients using equation (3) for field dependent charge mobilities as indicated by the solid line. The extraction field associated to determined mobility values was calculated as  $E^* = U't_{\text{max}}/d$  (squares),  $E^* = 0.65 \cdot U't_{\text{max}}/d$  (circles) or using the iterative procedure as described in the text (triangles).

of  $\mu$  and  $t_{\text{max}}$  values via equation (3), (2.) determine preliminary parameters  $\mu_0^{(0)}$  and  $\kappa^{(0)}$  from the measurement using  $E^* = U't_{\text{max}}/d$ , (3.) for each  $U'$ , calculate the theoretical CELIV transient from equation (9), numerically evaluate  $(\Delta j/j(0))^{\text{th}}$ ,  $t_{\text{max}}^{\text{th}}$  and  $\mu^{\text{th}}$  using equation (3) and calculate  $\delta = d \ln(\mu^{\text{th}}/\mu_0^{(0)})/U't_{\text{max}}^{\text{th}}\kappa^{(0)}$ , (4.) associate each *measured* mobil-

ity value to the extraction field  $E^* = \delta U' t_{\max}/d$  and determine optimized  $\mu_0^{(1)}$  and  $\kappa^{(1)}$  from this data, (5.) iterate the procedure by repeating steps 3 and 4 until the determined  $\mu_0^{(n)}$  and  $\kappa^{(n)}$  stabilize. This procedure is only moderately complex but significantly enhances the accuracy of charge mobility determination, at least when Poole-Frenkel field dependence prevails. Figure 9 shows that the results of this iteration procedure accurately track the true field-dependent mobility used for the simulated CELIV experiments.

## V. CONCLUSION

In this publication, we pointed out several difficulties that arise when applying the CELIV technique under the non-idealized conditions usually encountered in experiments. We based our analysis upon a rederivation of the original CELIV analysis, correcting for inaccuracies in the original publications that result in erroneous charge mobilities under conditions of high charge density. In the case of photogenerated charge carriers, we found a significant departure from the equilibrium assumption of the original derivations. The impact of bimolecular charge recombination on CELIV transients and their analysis in this situation has not been considered up to now. We showed that high charge densities as typically used in the experiments leads to an artificial time dependence of the determined mobility values. We were able to relate the experimental results for a M3EH-PPV/CN-ether-PPV blend solar cell solely to this effect, showing that the charge mobility is actually constant shortly after photoexcitation. Sufficient information was provided to facilitate an interpretation of experiments under conditions of non-equilibrium charge carrier extraction. As another strong deviation from idealized conditions we investigated the effect of field-dependent charge carrier mobilities. We showed that association of the CELIV mobilities with the electric field present at the time of extraction current maximum leads to significant errors in the determined field dependence. An optimized choice of the correlated extraction field was introduced, which yields much lower errors compared to the standard approach. Additionally, we showed that under the presumption of a Poole-Frenkel type field dependence, an iterative procedure can be applied to determine the true mobility-field dependence in a precise way.

## Acknowledgments

S. B. acknowledges financial support by the German Federal Ministry of Science and Education (BMBF FKZ 13N8953 and 03X3525D). M. Sch. acknowledges financial support by the German Research Foundation (DFG SPP 1355).

---

\* Electronic address: sbange@uni-potsdam.de

- <sup>1</sup> G. Juska, K. Arlauskas, M. Viliunas, and J. Kocka, Physical Review Letters **84**, 4946 (2000).
- <sup>2</sup> G. Juska, K. Arlauskas, M. Viliunas, K. Genevicius, R. Österbacka, and H. Stubb, Physical Review B **62**, R16235 (2000).
- <sup>3</sup> G. Juska, K. Genevicius, R. Osterbacka, K. Arlauskas, T. Kreouzis, D. D. C. Bradley, and H. Stubb, Physical Review B **67**, 081201(R) (2003).
- <sup>4</sup> K. Genevicius, R. Osterbacka, G. Juska, K. Arlauskas, and H. Stubb, Synthetic Metals **137**, 1407 (2003).
- <sup>5</sup> A. J. Mozer, N. S. Sariciftci, A. Pivrikas, R. Österbacka, G. Juska, L. Brassat, and H. Bässler, Physical Review B **71**, 035214 (2005).
- <sup>6</sup> R. Österbacka, A. Pivrikas, G. Juska, K. Genevicius, K. Arlauskas, and H. Stubb, Current Applied Physics **4**, 534 (2004).
- <sup>7</sup> A. J. Mozer, G. Dennler, N. S. Sariciftci, M. Westerling, A. Pivrikas, R. Österbacka, and G. Juska, Physical Review B **72**, 035217 (2005).
- <sup>8</sup> C. Yin, M. Schubert, S. Bange, B. Stiller, M. Castellani, D. Neher, M. Kumke, and H. H. Hörhold, Journal of Physical Chemistry C **112**, 14607 (2008).
- <sup>9</sup> M. Schubert, C. Yin, M. Castellani, S. Bange, T. L. Tam, A. Sellinger, H.-H. Hörhold, T. Kietzke, and D. Neher, Journal of Chemical Physics **130**, 094703 (2009).
- <sup>10</sup> B. Homa, M. Andersson, and O. Inganäs, Organic Electronics **10**, 501 (2009).
- <sup>11</sup> G. Juska, M. Viliunas, K. Arlauskas, N. Nekrasas, N. Wyrsh, and L. Feitknecht, Journal of Applied Physics **89**, 4971 (2001).
- <sup>12</sup> G. Juska, N. Nekrasas, K. Genevicius, J. Stuchlik, and J. Kocka, Thin Solid Films **451-452**, 290 (2004).
- <sup>13</sup> A. J. Mozer, N. S. Sariciftci, L. Lutsen, D. Vanderzande, R. Österbacka, M. Westerling, and

- G. Juska, Applied Physics Letters **86**, 112104 (2005).
- <sup>14</sup> P. Langevin, Annales De Chimie Et De Physique **28**, 433 (1903).
- <sup>15</sup> K. Genevicius, R. Osterbacka, G. Juska, K. Arlauskas, and H. Stubb, Thin Solid Films **403**, 415 (2002).
- <sup>16</sup> A. Pivrikas, N. S. Sariciftci, G. Juska, and R. Österbacka, Progress in Photovoltaics **15**, 677 (2007).
- <sup>17</sup> H. Bässler, Physica Status Solidi B **175**, 15 (1993).
- <sup>18</sup> G. Juska, K. Genevicius, K. Arlauskas, R. Osterbacka, and H. Stubb, Physical Review B **65**, 233208 (2002).